Applied Surface Science 271 (2013) 223–227

Contents lists available at SciVerse ScienceDirect

Applied Surface Science

journal homepage: www.elsevier.com/locate/apsusc

Characterization of direct- and back-scribing laser patterning of SnO_2:F for a-Si:H PV module fabrication

D. Canteli[a,*], I. Torres[a], J.J. García-Ballesteros[b], J. Cárabe[a], C. Molpeceres[b], J.J. Gandía[a]

[a] División de Energías Renovables, Energía Solar Fotovoltaica, CIEMAT, Avda. Complutense, 22, 28040, Madrid, Spain
[b] Centro Láser, Universidad Politécnica de Madrid, Ctra. de Valencia Km, 7.3, 28031, Madrid, Spain

ARTICLE INFO

Article history:
Received 13 June 2012
Received in revised form 15 January 2013
Accepted 23 January 2013
Available online 31 January 2013

Keywords:
Laser processing
Transparent conductive oxide
Fluorine-doped tin oxide

ABSTRACT

In thin film photovoltaic modules, the different solar cells are interconnected monolithically during the production process, which gives a greater control over the size and output characteristics of the finished module. The interconnection is typically achieved through different laser scribing processes made at different production steps. In thin film modules built in the superstrate configuration, the first laser process is the patterning of the transparent front electrode. This paper presents results on the investigation of this first laser scribing process on fluorine-doped tin oxide deposited onto a glass substrate using nanosecond diode-pumped solid-state laser sources. Processes made with two different wavelengths (1064 nm and 355 nm) and executed from the film-side and from the substrate side are compared and evaluated. The quality of the scribes is assessed with confocal and scanning electron microscopy images. In addition, Raman microscopy is used to study the extension of the heat affected zones. While good quality scribes were obtained using both wavelengths and either film-side or substrate-side irradiation, only using 355 nm and substrate-side scribing yielded grooves with no observable heat affected zones. It also needed the lowest values of energy per ablated volume and allowed for the highest processing speeds. As such, substrate side ablation with 355 nm is proposed as the best ablation strategy.

1. Introduction

Fluorine-doped tin oxide (SnO_2:F) is an excellent transparent conductive oxide (TCO) widely used in optoelectronic devices. It is especially suitable for the fabrication of thin film photovoltaic devices since it possess some remarkable properties such as a high transmittance in the visible range of the electromagnetic spectra, a low sheet resistance and a high chemical stability at moderately elevated temperatures [1–3].

In thin film photovoltaic modules, the different solar cells are connected in series monolithically during the fabrication process. To achieve this, different grooves, commonly called P1, P2 and P3 are introduced to obtain an electrical connection between the front contact of a cell and the back contact of the adjacent cell. Since laser processes can be used to obtain clean and narrow grooves, laser scribing has established as the industry standard method to perform the scribes [4–7].

In devices constructed in the superstrate configuration, the different layers are deposited onto a transparent substrate which serves as the supporting structure and as a window for the device illumination. After the deposition of a TCO onto the glass substrate, P1 scribes are made to divide the TCO into electrically isolated stripes. The number and width of these stripes define the number and width of the module' solar cells. This laser process is usually executed from the film side using an infrared (IR) or an ultraviolet (UV) nanosecond (ns) laser source.

Material ablation with ns laser sources, especially when using IR radiation, is fundamentally a thermal ablation process. In semiconductors, such as tin oxide, IR laser light excites electrons in the material conduction band and the energy of these excited electrons is almost instantly transferred to the material net. On the other hand, in the ablation of materials with UV laser sources intra-band transitions and excitation of defect states or even direct bond breaking can occur if the material has an energy gap similar to the energy of the laser source. If the relaxation time of these excited species is comparable to the characteristic desorption time of excited atoms or electrons, mechanism like material desorption or spallation can contribute to the ablation [8].

The ablation of thin films deposited onto transparent substrates can be carried out directly from the film side or irradiating through the substrate side by an induced process. The ablation mechanism in both cases can be different. Film-side laser ablation is usually driven by absorption, heating, and heat transport with subsequent

* Corresponding author. Tel.: +34 913466039.
E-mail address: david.canteli@ciemat.es (D. Canteli).

0169-4332/$ – see front matter © 2013 Elsevier B.V. All rights reserved.
http://dx.doi.org/10.1016/j.apsusc.2013.01.164

melting and evaporation of the illuminated material. But when the film is removed irradiating from the substrate side, the process is not necessarily purely governed by thermally affecting (heating, melting, and evaporating) the complete layer. Instead, it is possible that only a fraction of the film close to the film/substrate interface is ablated through the absorption of the incident radiation. For high enough energies, the subsequent developed stress at the film/substrate interface can be sufficient to lift up the whole film [4,9].

In this work, we employed two different wavelengths in the UV and IR part of the spectrum (1064 nm and 355 nm) to study the removal of SnO_2:F deposited onto glass substrates. Additionally, two different irradiation geometries were studied, i.e. irradiating from the film side and from the substrate side. Craters and complete P1 scribes susceptible of being used in the fabrication of thin film PV modules were achieved with both wavelengths and both irradiation configurations. Based on the morphology of craters created with single pulses and of complete scribes, we proposed different removal processes depending on the wavelength used and on the irradiation geometry. Additionally, using Raman spectroscopy, we evaluated the heat affected zone generated during the process. Finally, according to the results gathered we comment on the preferable wavelength and irradiation geometry for the fabrication of P1 scribes.

2. Materials and methods

2.1. Laser sources

The laser sources used in this work were ns Gaussian diode-pumped solid-state lasers (Nd:YVO_4) from Spectra Physics. For ablation at IR, the laser operated at the fundamental frequency of 1064 nm. The laser repetition frequency could be varied between 1 kHz and 100 kHz. The maximum average power was about 4.8 W and the beam had a quality factor $M^2 < 1.15$. The laser source was positioned directly over the sample which was placed on a stage driven by three electro-mechanical axis that allowed sample movement at speeds up to 5 m/s.

For the UV ablation, the 1064 nm laser frequency was tripled to 355 nm. The laser repetition frequency could be varied between 15 kHz and 300 kHz. The maximum average power was about 3.5 W and the beam had a quality factor $M^2 < 1.3$. In this case, the laser beam was led and focused on the sample surface by an optical system that included two mirrors, a beam expander, a digital scanner that allowed scanning speeds up to 10 m/s (HurryScan II 14, Scanlab,) and a lens with a 250 mm focal length.

The beam waist of both lasers was calculated following the method described by Liu [10]. Because of the optical differences in the laser systems for each wavelength, the lasers beam' waist and depth of field were different. The obtained beam waists were approximately 20 μm for the IR laser and about 35 μm for the UV laser. Moreover, the IR laser had a very small depth of field (less than 1 mm) which made the laser processes very sensible to the sample position. To compare the pulses emitted by both lasers the pulses' peak fluence was used.

All the experiments were carried out with the sample positioned approximately in focus. The focus position was estimated by examining marks created in the samples at different distances from the lens by single, low-energy laser pulses. This was done for both wavelengths and for film- and substrate-side irradiation. The focus position would be located approximately where the mark was smallest. With this approach, the change in the focus position due to the refraction suffered by the laser beam when going through the glass in substrate side irradiation was adjusted.

2.2. Samples and material characterization

For this study we used samples of a commercial TCO based on SnO_2:F (Asahi® U-type) [2,3]. The films had a thickness of 850 nm and had its surfaces texturized (rms roughness ~30–50 nm as measured from confocal images) to improve light trapping. Optical transmittance and reflectance of the SnO_2:F films were obtained with a PerkinElmer Lambda 1050 UV/Visible/NIR. The morphological characterization of the laser pulses and grooves was done with a confocal microscope (Leica DCM 3D) and scanning electron microscopy (SEM) (HITACHI S-3500 N). To study possible material modifications caused during the laser process, we measured EDX and Raman spectra using the 514.5 nm line of an Ar laser (InVia Renishaw) in the vicinity of the ablated zone. The electrical isolation of the P1 scribes was checked using a common multimeter (range up to 550 MΩ).

3. Results and discussion

3.1. Single pulse removal

To study the removal of the SnO_2:F films when using IR and UV wavelengths and for film- and substrate-side irradiation, experiments using single laser pulses were performed first. Since the two lasers have different wavelengths and beam radius, some differences appeared when ablating the TCO. For example, using the method described by Liu [10] we calculated the damage threshold of the material and the obtained values for film side irradiation were 1.7 J/cm^2 at 355 nm and 1.1 J/cm^2 at 1064 nm. In Fig. 1 SEM images of the craters obtained with the different wavelengths and different irradiation geometries are shown.

When the film was irradiated with 1064 nm from the film side (Fig. 1a), fluence values around 1.6 J/cm^2 were enough to remove the whole film. The obtained craters presented very smooth edges and walls evidencing the melting and posterior solidification of material. On the other hand, when using 355 nm irradiating from the film side, the morphology of the craters obtained showed a very irregular surface, evidencing an inhomogeneous ablation (See Fig. 1b). Yet, it was still possible to distinguish traces of molten and re-solidified material in the surface of the craters. At pulse fluence values of about 1.8 J/cm^2 the craters reached an average depth of approximately 650 nm and the use of higher fluence values (up to 11 J/cm^2) did not produce deeper craters.

The strong differences in the crater morphology indicated different ablation mechanisms. With 1064 nm, the morphology obtained was typical of a thermal mechanism where the material is melted and evaporated as a consequence of the energy transferred to the material by the electrons excited with the IR light. On the other hand, the morphology of the craters obtained with 355 nm suggested that the ablation mechanism probably involved bond breaking processes and material ejection in addition to the thermal processes involved in ns laser-matter interactions. The fact that the whole film could not be ablated at the highest fluence values (11 J/cm^2) suggested that the UV light was highly absorbed as it penetrated the material.

When irradiating from the substrate side, a fluence value of 2.1 J/cm^2 was needed to remove completely the TCO film with IR light whereas 1.5 J/cm^2 was enough when using UV light. The obtained crater morphology was very different in each case. The craters obtained with 1064 nm from the substrate side (Fig. 1c) were very similar to those executed from the film side (Fig. 1a) suggesting that the same removal mechanism applied to both cases. Since IR light is absorbed more homogeneously throughout the whole film's thickness than UV light, the irradiation geometry did not play a determining role. On the other hand, the craters obtained

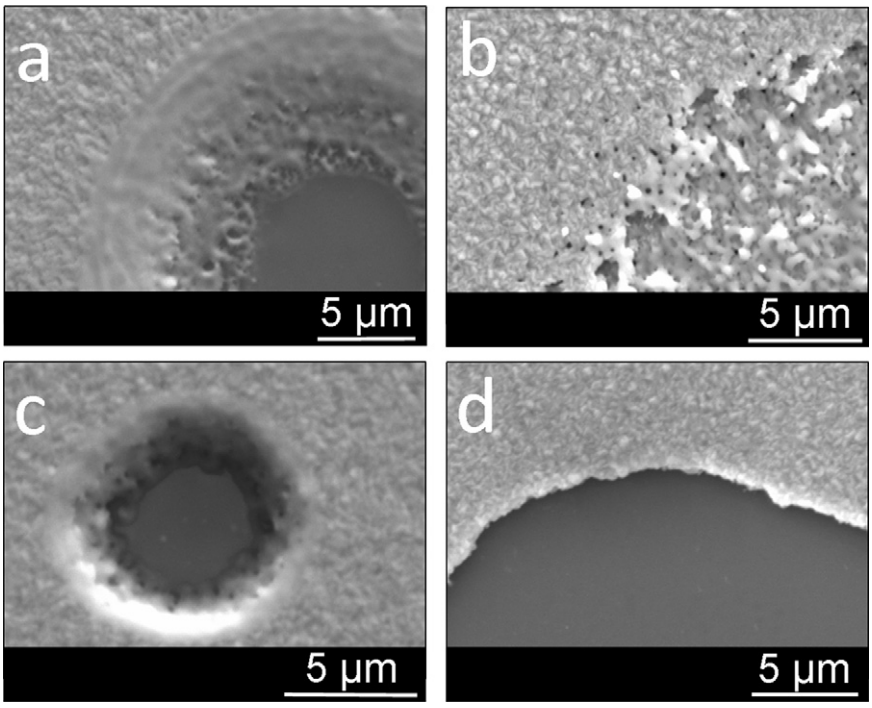

Fig. 1. Detailed SEM images of single laser pulses with: (a) 1064 nm laser from the film side; (b) 355 nm laser from the film side; (c) 1064 nm laser from the substrate side; (d) 355 nm laser from the substrate side.

with 355 nm light from the substrate side had a very sharp edge without signs of thermal fusion (Fig. 1d). This is typical of the mechanical rupture of the film seen in an induced removal mechanism [9]. Hence, it was reasonable to conclude that UV light was mainly absorbed near the material/substrate interface and that the build up pressure due to the evaporation of the first nm of material was sufficient to break and eject the whole film thickness.

3.2. P1 grooves

The final objective of this work was to compare the effects of both wavelengths and both irradiation geometries on the quality of P1 grooves. In particular, we were looking to achieve P1 scribes with good electrical and morphological properties while using the minimum energy necessary and the fastest speed possible.

As described in the previous section, the TCO film can be removed completely with a single pulse using UV light from the substrate side or IR light from either the film or substrate side. Therefore, using a fluence value high enough to ablate the TCO film and an overlap high enough to connect the craters obtained with each pulse should have yielded continuous grooves. The overlap in the different scribes was defined from the size of a single pulse crater, D, using the following expression:

$$\text{Overlap}\,(\%) = 1 - \frac{v}{Df}$$

In this expression, v is the process speed and f the repetition frequency.

When irradiating with UV light from the film side several pulses were needed to remove the TCO film. Therefore, the overlap value cannot be defined in terms of the diameter of a single pulse crater. Accordingly, we have replaced D in the previous expression by the groove's width.

Following the approach of minimum fluence and overlap values, it was possible to create scribes with a morphology suited for its application to thin film photovoltaic modules i.e. flat bottoms, smooth walls and no shoulders or spikes in the grooves' edges (as observed from confocal and SEM images) with UV light irradiating from the substrate side (Fig. 2d) and with IR light irradiating from the film- (Fig. 2a) and substrate-side (Fig. 2c). shows as an example four representative working grooves made using the different wavelengths and irradiation approaches tested. It is worth noting that both laser systems had different focusing optics and different scanning speeds. The differences in the grooves' width are most likely influenced by this. We could not discern any damage to the substrate in the confocal and SEM images either. However, it was found that with the procedure of using minimum fluence and overlap values, only the scribes done with 355 nm and irradiating from the substrate side (Fig. 2d) fulfilled the requirement of high electrical isolation. In the other two cases, higher fluences or higher overlap values were needed to obtain high electrical resistances. For example, when using IR light irradiating from the film (Fig. 2a) or from the substrate side (Fig. 2c), fluence values as high as 10 J/cm^2 were needed to electrically isolate the scribes at low pulse overlaps (~25%). If we increased the pulse overlap, lower fluence values (3.3 J/cm^2 at 70% overlap for example) could be used in detriment of a lower process speed. These results could be explained in terms of the different mechanisms proposed for single pulse removal. The processes achieved with IR light clearly showed signs of melted and re-solidified material (Fig. 2a and c). Although from the images the bottom of the grooves seemed completely clean, certainly some materials remnants coming from the molten mixture must have been present. Hence, higher fluence values or higher pulse overlap than expected were needed to completely remove the film and achieve electrical isolation. Finally, in the case of UV light irradiating from the film side we have shown that it was not possible to remove the entire film with single laser pulses. Therefore, very high overlaps (>90%) were needed to achieve electrical isolation with the scribe even at fluence values of 10 J/cm^2. This resulted in wider grooves, with wider and less vertical walls, and a slight elevation of the grooves edges (Fig. 2b).

Table 1 shows the fabrication parameters for the grooves obtained with the lowest energy/ablated volume (most efficient processes). The ablated volume of a groove can be calculated from

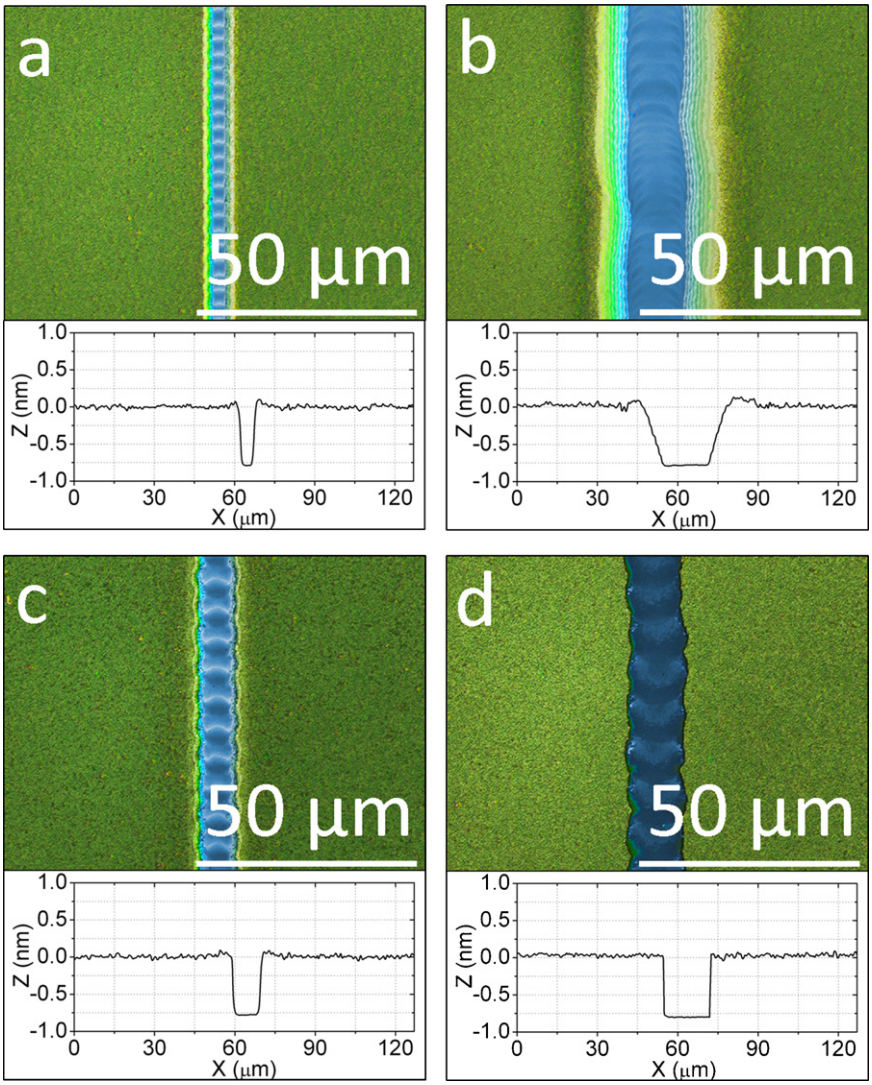

Fig. 2. Confocal images and profiles of P1 functional grooves made at different conditions: (a) 1064 nm, film side (20 kHz 102 mW 90 mm/s); (b) 355 nm, film side (20 kHz 274 mW 61 mm/s); (c) 1064 nm, substrate side (20 kHz 132 mW 180 mm/s); (d) 355 nm, substrate side (20 kHz 132 mW 246 mm/s).

confocal images or from a simple relation between the average power, the speed used and the width and depth of the grooves [4]. Since the grooves studied were very clean, both methods yielded similar results. Accordingly with the single pulse results, a lower energy was needed to ablate the material when scribing from the substrate side with a 355 nm laser, making this approach the most favourable from an energetic point of view.

3.3. Material modifications

In order to study possible changes produced in the material structure due to the laser interaction, EDX and Raman spectra were measured at different points: the glass substrate, the TCO surface and at several points at different distances from the groove edge.

Fig. 3 shows an example of the Raman spectra measured. The spectra obtained in point 1 and point 2, which were points located inside the groove, are characterized by having a broad band ranging from 530 cm^{-1} to 670 cm^{-1} that can be assigned to the glass substrate. None of the active Raman modes typically observed in SnO_2 samples were present in those two spectra. On the other hand, the spectra measured in points 3–5 and surface, revealed the typical features found in Raman spectra of SnO_2 samples. The peaks located in 638 cm^{-1} and 776 cm^{-1} can be assigned to the $A1_g$ and $B2_g$ vibration modes of SnO_2 while the broad band located around 465 cm^{-1} can be attributed to the $E1_g$ mode [1,2]. The spectra in points 3–5 and surface also presented two more peaks in 240 cm^{-1} and 280 cm^{-1} that are not generally found in spectra taken in SnO_2 samples. These peaks have not been identified, but

Table 1
Example of parameters and groove characteristics of process performed with 355 nm and 1064 nm laser light from both the film side and substrate side.

	Repetition frequency (Hz)	Pulse energy (J)	Fluence (J/cm^2)	Process speed (mm/s)	Overlap (%)	Groove width (µm)	Energy/Ablated volume (J/mm^3)
355 nm film-scribing	60,000	3.98×10^{-6}	0.9	102	92.8	23.7	143
355 nm substrate-scribing	100,000	4.90×10^{-6}	1.1	1020	27.1	14.0	41
1064 nm film-scribing	50,000	6.80×10^{-6}	4.3	350	27.0	9.6	206
1064 nm substrate-scribing	20,000	1.42×10^{-5}	9.0	180	37.1	14.3	164

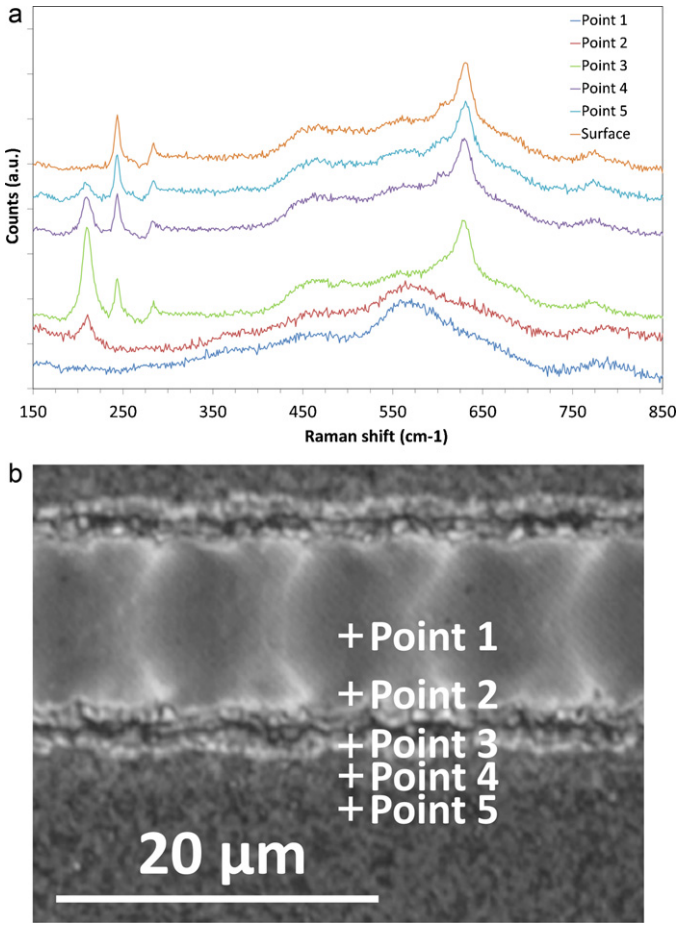

Fig. 3. Raman spectra (a) in different points (b) over a P1 scribe performed from the substrate side with a 1064 nm laser. A peak at 211 cm^{-1} could be observed, showing an affected area near the groove edge.

appear in spectra taken in other fluorine doped tin oxide samples [2] and, therefore, could be originated by the fluorine impurities.

In addition, in the spectra taken in points 2–5, i.e. in the vicinity of the grooves edge, there is another peak located in 211 cm^{-1}. This peak can be ascribed to the $A1_g$ mode of tin monoxide (SnO) [11]. If the spectra was taken farther away from the scribe edge (as in the surface spectra in Fig. 3.) the peak disappeared. Likewise, that peak was not detected in the spectra taken in any location in scribes executed with 355 nm irradiating from the substrate side. Hence, the presence of SnO could be related to a thermal effect produced by the laser that extends about five microns away from the groove and that is absent in the scribes obtained through an induced removal mechanism. That peak was also observed in point 2 in some grooves. Since no other peaks were detected in those spectra, its presence was related to the re-deposition of the removed material.

Finally, EDX spectra were measured at similar points as the Raman spectra, but no differences were observed between the affected area and the TCO surface far from the grooves. Furthermore, stoichiometry calculations were made from the spectra revealing no significance differences in the amount of tin measured.

As the main objective of the P1 grooves is to electrically isolate the different solar cells, the material modification observed did not affect the groove function. Nevertheless, the extension of the affected area was too small to possibly influence module performance.

4. Conclusions

IR and UV laser ablation from the film side and from the substrate side of fluorine-doped tin oxide films deposited onto a glass substrate were studied. When irradiating with IR light from the film and from the substrate side, the observed craters' morphology was typical of a thermal ablation mechanism, i.e. very smooth features due to melted and re-solidified material. In fact, from the study of P1 scribes, it was concluded that melted material was re-deposited in the grooves bottom and, in order to make isolating scribes, high pulses overlap were needed.

On the other hand, the craters obtained with UV light irradiating from the film side had very irregular features. The UV light was also highly absorbed by the film, and even when using fluence values as high as 11 J/cm^2 several laser pulses were needed to remove the entire film. Therefore, in order to make isolating P1 grooves, very high overlaps were necessary. Finally, if the film was irradiated with UV light from the substrate side, it was removed through an induced mechanism leaving very clean craters, with very sharp edges. With this approach, it was possible to obtain P1 grooves with the lowest pulse overlap and pulse energy.

From Raman spectra, we identified an affected area extending several μm at the sides of the laser grooves. This material modification was not observed in processes performed by induced ablation (355 nm from the substrate side) and hence was attributed to a thermal modification of the material.

P1 grooves made with UV light irradiating from the substrate side is proposed as the preferred method since it allowed for the fastest processing speeds while using the lowest energy/ablated volume and showed no evidence of thermal damage in the surroundings of the grooves.

Acknowledgement

Partial financial support for this work has been provided by the Spanish Ministry of Economy and Competitiveness under the projects AMIC (ENE2010-21384-C04-01) and INNDISOL (IPT-420000-2010-6).

References

[1] M. Batzill, U. Diebold, The surface and materials science of tin oxide, Progress in Surface Science 79 (2005) 47–154.
[2] R. Chandrasekhar, K.L. Choy, Electrostatic spray assisted vapour deposition of fluorine doped tin oxide, Journal of Crystal Growth 231 (2001) 215–221.
[3] K. Sato, K. Adachi, Y. Hayashi, M. Mizuhashi, Hydrogen plasma durability of SnO2:F films for use in a-Si solar cells, in: Photovoltaic Specialist Conference, 1998, pp. 267–272.
[4] G. Heise, M. Dickmann, M. Domke, A. Heiss, T. Kuznicki, J. Palm, I. Richter, H. Vogt, H.P. Huber, Investigation of the ablation of zinc oxide thin films on copper–indium–selenide layers by ps laser pulses, Applied Physics A 104 (2011) 387–393.
[5] Q. Qiao, K. Ma, Y.Q. Wang, G.C. Zhang, Z.R. Shi, G.H. Li, Optimization of laser patterning of textured gallium-doped zinc oxide for amorphous silicon photovoltaics, Applied Surface Science 256 (2010) 4656–4660.
[6] J.J. García-Ballesteros, I. Torres, S. Lauzurica, D. Canteli, J.J. Gandía, C. Molpeceres, Influence of laser scribing in the electrical properties of a-Si:H thin film photovoltaic modules, Solar Energy Materials and Solar Cells 95 (2011) 986–991.
[7] S. Lauzurica, J.J. García-Ballesteros, M. Colina, I. Sánchez-Aniorte, C. Molpeceres, Selective ablation with UV lasers of a-Si:H thin film solar cells in direct scribing configuration, Applied Surface Science 257 (2011) 5230–5236.
[8] D. Bäuerle, Laser Processing and Chemistry, fourth ed., Springer-Verlag, Berlin Heidelberg, 2011.
[9] G. Heise, M. Domke, J. Konrad, S. Sarrach, J. Sotrop, H.P. Huber, Laser lift-off initiated by direct induced ablation of different metal thin films with ultra-short laser pulses, Journal of Physics D: Applied Physics 45 (2012) 315303.
[10] J.M. Liu, Simple technique for measurements of pulsed Gaussian-beam spot sizes, Optics Letters 7 (1982) 196–198.
[11] S. Koval, R. Burriel, M.G. Stachiotti, M. Castro, R.L. Migoni, M. Moreno, A. Varela, C.O. Rodriguez, Linear augmented-plane-wave frozen-phonon calculation, shell-model lattice dynamics, and specific-heat measurement of SnO, Physical Review B 60 (1999) 14496–14499.